

# Visualizing classical and quantum probability densities for momentum using variations on familiar one-dimensional potentials

R. W. Robinett\*

*Department of Physics*

*The Pennsylvania State University*

*University Park, PA 16802 USA*

(Dated: June 4, 2022)

## Abstract

After briefly reviewing the definitions of classical probability densities for position,  $P_{CL}(x)$ , and for momentum,  $P_{CL}(p)$ , we present several examples of classical mechanical potential systems, mostly variations on such familiar cases as the infinite well and the uniformly accelerated particle for which the classical distributions can be easily derived and visualized. We focus especially on a simple potential which interpolates between the symmetric linear potential,  $V(x) = F|x|$ , and the infinite well, which can illustrate, in a mathematically straightforward way, how the divergent,  $\delta$ -function classical probability density for momentum for the infinite well can be easily seen to arise. Such examples can help students understand the quantum mechanical momentum-space wavefunction (and its corresponding probability density) in much the same way that other semiclassical techniques, such as the WKB approximation, can be used to visualize position-space wavefunctions.

---

\*Electronic address: rick@phys.psu.edu

# 1. Introduction

Since the introduction of quantum mechanics early in the last century, practitioners and students of the subject alike have used semi-classical methods to calculate, understand, and visualize properties of position-space solutions of the time-independent Schrödinger equation. WKB-type solutions [1], for example, provide an attractive and mathematically understandable approximation which makes manifest the typical correlations between the magnitude of a stationary state wavefunction and the corresponding 'wiggleness'. At a somewhat less sophisticated level, many textbooks [2], [3], make direct comparisons between the quantum mechanical probability density, defined by  $P_{QM}(x) = |\psi(x)|^2$ , with intuitively derived classical counterparts,  $P_{CL}(x)$ , which are often motivated by very simple '*how much time is spent in a given interval*' arguments.

In comparison, there are far fewer discussions in the pedagogical literature or in standardly used textbooks giving examples of the corresponding semi-classical connections to momentum-space solutions,  $\phi(p)$ . Solutions to the Schrödinger equation obtained directly from a momentum-space formulation (such as for the uniformly accelerated particle) are sometimes presented, but most often the information encoded in  $\phi(p)$  is simply noted to be related to that in the position-space wavefunction by a rather formal operation, namely the Fourier transform, via

$$\phi(p) = \frac{1}{\sqrt{2\pi\hbar}} \int_{-\infty}^{+\infty} \psi(x) e^{ipx/\hbar} dx. \quad (1)$$

Correlating the information clearly evident in the magnitude/wiggleness of a position-space,  $\psi(x)$ , with the similar information encoded in  $\phi(p)$  is a non-trivial task, even for experienced scientists, and students first approaching the subject often can find no obvious connections between the form of the quantum mechanical probability density for momentum,  $|\phi(p)|^2$ , and their intuition about classical mechanics. A recent study [4] of the progression of student understanding of quantum mechanical concepts, starting with introductory modern physics courses, through advanced undergraduate quantum mechanics classes, to first year graduate quantum theory courses, has provided evidence that while student understanding of the form of position-space wavefunctions does increase through the undergraduate curriculum, their ability to extend these notions to momentum-space ideas lags far behind.

Finally, since the results of experiments from a wide variety of areas in physics are increasingly presented in the form of momentum distributions [5], [6], a background in un-

derstanding a momentum-space approach to classical and quantum mechanics is becoming more important for students to acquire.

Motivated by all of these factors, in this note we will discuss several simple model systems for which one can rather easily calculate, analyze, and visualize the classical probability densities for both position and momentum, and to also compare them directly to their quantum mechanical equivalents to visualize the correspondence principle limit in both  $x$ - and  $p$ -space. We first briefly review, in Sec. 2, the basic definitions of classical probability densities for one-dimensional bound state problems and apply these methods to the simple problem of the 'bouncer', a particle subject to a uniform gravitational force, but with a rigid, infinite wall constraint due to a horizontal surface. As our main example, in Sec. 3, we provide an attractive interpolating case which shows how both the classical and quantum mechanical descriptions for the symmetric linear well (defined by  $V(x) = F|x|$  and hence related to the 'bouncer' or uniform acceleration case) and the standard infinite well potentials can be smoothly connected to one another, and how the classical momentum distributions can be easily extracted. we also show, in some detail, how the magnitude/wiggleness of the position space quantum wavefunction is directly correlated to the form of its momentum-space  $\phi(p)$  transform. This last case also provides an intuitively clear and mathematically appropriate description of how the limiting case of the divergent,  $\delta$ -function momentum-space classical probability densities can arise for the infinite well case.

## 2. Review of classical probability densities for position and momentum: the 'bouncer' as an example

In order to review the calculation and visualization of classical probability densities for position,  $P_{CL}(x)$ , and momentum  $P_{CL}(p)$ , we begin by illustrating, in Fig. 1, a rather generic potential energy function,  $V(x)$  versus  $x$ , which can give rise to bound states which can be described either classically or quantum mechanically. A fixed value of the energy  $E$  is shown which then defines the classical turning points,  $a$  and  $b$ , defined by  $V(a) = E = V(b)$ : this implies that  $P_{CL}(x)$  will be non-vanishing only over the range  $(a, b)$ . The corresponding range in allowed momentum values are given by conservation of energy using

$$p(x) = \pm \sqrt{2m(E - V(x))} \quad \text{giving} \quad p_m \equiv \sqrt{2m(E - V_{min})} \quad (2)$$

so that the classical probability density,  $P_{CL}(p)$ , will be defined over the range  $(-p_m, +p_m)$ .

The variation of momentum values with position in the potential well is perhaps best shown in a phase-space  $x - p$  plot, also included in Fig. 1, which simultaneously illustrates the allowed ranges in both variables.

We note that a particle at a given  $x$  location will experience both positive ( $+p(x)$ ) and negative ( $-p(x)$ ) values with equal probability as it moves from left to right and then back from right to left. Thus, even if the potential energy function is not symmetric, the classical probability density for momentum,  $P_{CL}(p)$ , will necessarily satisfy  $P_{CL}(-p) = P_{CL}(+p)$ . This feature is also echoed in the  $x - p$  plot in Fig. 1 where the phase-space curve need not be symmetric about any vertical axis, but will necessarily be symmetric about the  $p = 0$  line.

We note from the figure that there may well be more than one location where the particle has the same momentum value, given by  $p = \sqrt{2m(E - V(x))}$ , such as at  $x = c$  and  $x = d$ . We must then take both contributions to  $P_{CL}(p)$  into account in the formalism which follows. One case in which this may not occur is if there is an infinite wall type potential barrier from which particles simply 'bounce' and rebound instead of slowing down on one side, coming instantaneously to rest, and then reversing direction as shown in the case in Fig. 1.

The classical motion in any such bound state system will be periodic with period  $T_{CL}$ , corresponding to a complete set of left to right and back to left (e.g.,  $a$  to  $b$  and then back to  $a$ ) motions. For some purposes, we only require the 'half-period' (the  $a$  to  $b$  time) given by  $\tau = T_{CL}/2$  and this quantity can be easily calculated from the potential energy function via

$$\tau = \int_{t_a}^{t_b} dt = \int_a^b \frac{dx}{v(x)} = \sqrt{\frac{m}{2}} \int_a^b \frac{dx}{\sqrt{E - V(x)}}. \quad (3)$$

A standard argument leading to the classical probability density for position,  $P_{CL}(x)$ , begins by noting that the small probability of finding the particle with position in the range  $(x, x + dx)$  should be proportional to the amount of time spent in that interval,  $dt$ . The fraction of time spent in that small interval will be  $dt/T_{CL}$  and using the definition of probability density, we find that

$$P_{CL}(x) dx \equiv d\text{Prob}[x, x + dx] = \frac{dt}{T_{CL}}. \quad (4)$$

We then recall that (i) the particle will be in the same  $dx$  bin on both its 'back' and 'forth' trips, so the last term should really be doubled, and (ii) the classical speed,  $v(x) = |dx/dt|$ ,

can be used to relate  $dx$  directly to  $dt$ , giving the familiar result

$$P_{CL}(x) = \frac{d\text{Prob}[x, x + dx]}{dx} = 2 \left( \frac{dt/T_{CL}}{dx} \right) = \frac{1}{\tau v(x)} \quad (5)$$

where  $\tau = T_{CL}/2$  is the 'half-period'. We note that Eqn. (3) ensures that this definition will give a  $P_{CL}(x)$  which is automatically normalized to unity.

A similar expression for the small probability that a measurement will find the particle with momentum values in the range  $(p, p + dp)$  is given by

$$P_{CL}(p) dp \equiv d\text{Prob}[p, p + dp] = \frac{dt}{T_{CL}} \quad (6)$$

and we need the definition of the classical force,  $|F| = |dp/dt|$ , to be able to write

$$P_{CL}(p) \equiv \frac{d\text{Prob}[p, p + dp]}{dp} = \frac{dt/T_{CL}}{dp} = \frac{1}{T_{CL}|F(p)|} \quad (7)$$

where we require the magnitude of the force, as a function of  $p$ . Depending on the nature of the potential, we may have to take two or more contributions into account when evaluating Eqn. (7), such as with the  $x = c, d$  points in Fig. 1 mentioned above.

As an example of a calculation and visualization of both  $P_{CL}(x)$  and  $P_{CL}(p)$  for a simple potential, we consider the classical 'bouncer', corresponding to a particle bouncing, without loss of energy, under the influence of gravity, over a rigid horizontal surface [7]. The corresponding potential energy function is given by

$$V(z) = \begin{cases} +\infty & \text{for } z < 0 \\ mgz & \text{for } z \geq 0 \end{cases} \quad (8)$$

If we imagine a point object with total energy  $E$ , the maximum height,  $H$ , (which is one turning point, in addition to  $z = 0$  where it 'bounces'), is given by  $E = mgH$ ; the maximum momentum magnitude,  $p_m$ , is given by  $E = p_m^2/2m$  or  $p_m = \sqrt{2mE}$ . The 'half-period',  $\tau$ , is simply the time it takes to fall through the distance  $H$ , namely  $\tau = \sqrt{2H/g}$  and  $T_{CL} = 2\tau$ . The position dependent speed is given  $v(z) = \sqrt{2/m}\sqrt{E - mgz}$  so that the classical position probability density is

$$P_{CL}(z) = \frac{1}{\tau v(z)} = \left[ \frac{1}{\sqrt{2H/g}} \right] \left[ \frac{1}{\sqrt{(2/m)(E - mgz)}} \right] = \frac{1}{2\sqrt{H(H - z)}} \quad (9)$$

which has an (integrable) divergence at  $z = H$  where the particle slows down and reverses direction, but is finite at  $z = 0$  where the particle simply 'bounces', reversing direction, but

with no change in speed. The corresponding classical probability density for momentum will be non-vanishing only over the range  $(-p_m, +p_m)$  and is given by

$$P_{CL}(p) = \frac{1}{T_{CL}|F(p)|} = \left[ \frac{1}{2\sqrt{2H/g}} \right] \left[ \frac{1}{mg} \right] = \frac{1}{2\sqrt{2m(mgH)}} = \frac{1}{2\sqrt{2mE}} = \frac{1}{2p_m} \quad (10)$$

corresponding to a 'flat' momentum distribution over the allowed range. For this potential, due to the infinite wall at  $z = 0$ , the momentum only achieves a particular value *once* during each complete cycle (and not at two separate locations, such as the  $x = c, d$  case in Fig. 1), so we only have one contribution to  $|F(p)|$ . (The quantum mechanical solutions, for both  $\psi(x)$  and  $\phi(p)$ , and their comparisons to the classical results, for a very similar problem are discussed, in details, in the next section.)

The expressions in Eqns. (9) and (10) for  $P_{CL}(x)$  and  $P_{CL}(p)$  can be visualized using a 'projection of trajectory' technique [8] which implements the definitions of the classical probability densities in Eqns. (4) and (6) involving 'time spent' arguments. We can use a typical solution to the 'bouncer' problem of the form

$$z(t) = v_0 t - gt^2/2 \quad \text{and} \quad v_z(t) = v_0 - gt \quad (11)$$

where  $v_0 = \sqrt{2gH}$  is the initial speed, corresponding to an object 'thrown upwards'; the motion then repeats itself after each classical period. In Fig. 2, on the respective vertical axes ( $z(t)$  and  $p_z(t) = mv_z(t)$ ), we indicate equal-sized bins ( $dz$  and  $dp$ ), project them horizontally until they intersect the trajectory curves, then 'drop down' to the  $t$  axes. The small amounts of time,  $dt$ , corresponding to each 'bin' in either  $z$  or  $p_z$  are then proportional to the probability in that interval and are shown (as a histogram) on the appropriate vertical axes. The characteristic peaking near  $z = H$  and the finite value at  $z = 0$  is evident for  $P_{CL}(z)$ , while the striking 'flat' momentum probability density is easily visualized using this technique. A number ( $N = 1000$ ) of random 'measurements' of the particle's position and momentum over a single classical period are also shown alongside the 'binned' probabilities (as dots) and reflect the same phenomena.

### 3. The infinite well as a limiting case

The most familiar of all quantum mechanical bound state problems, the infinite well, can also be used an example of classical and quantum mechanical probability densities for

momentum. We will also discuss a very useful interpolation between the symmetric linear well, defined by the potential  $V(x) = F|x|$  (and hence analogous to the 'bouncer'), and the standard infinite well which can be used to show how the position- and momentum-space distributions smoothly go from one limit to the other. We first recall that if we define the infinite potential with walls at  $x = \pm a$ , via

$$V(x) = \begin{cases} +\infty & \text{for } |x| > a \\ 0 & \text{for } |x| < a \end{cases} \quad (12)$$

the classical speed and 'half-period' are trivially related to the total energy via  $v = \sqrt{2E/m}$  and  $\tau = 2a/v$  so that the classical probability density for position is given

$$P_{CL}(x) = \frac{1}{\tau v(x)} = \frac{1}{2a} \quad (13)$$

independent of  $E$  and determined solely by the geometry of the well. The energy eigenstates for the corresponding quantum mechanical problem can be characterized by parity with, for example, the even states being given by

$$\psi_n^{(+)}(x) = \frac{1}{\sqrt{a}} \cos\left(\frac{(n-1/2)\pi x}{a}\right) \quad \text{with energies} \quad E_n^{(+)} = \frac{\hbar^2(n-1/2)^2}{8ma^2} \quad (14)$$

and similar expressions for the odd states. For large values of  $n$ , the quantum mechanical probability density,  $P_{QM}(x) = |\psi_n^{(+)}(x)|^2$ , locally averages to the classical result, since  $\langle \cos^2(z) \rangle = 1/2$ .

The classical momentum probability density can be easily described in words as consisting of equal probabilities of finding the particle with momentum values given by  $\pm p_0 = \pm\sqrt{2mE}$ , which one can write in the form

$$P_{CL}(p) = \frac{1}{2} [\delta(p - p_0) + \delta(p + p_0)] . \quad (15)$$

The corresponding quantum mechanical solutions mimic this 'twin peaks' structure as one can see by calculating the momentum-space wave function for the even case, e.g.

$$\begin{aligned} \phi_n^{(+)}(p) &= \frac{1}{\sqrt{2\pi\hbar}} \int_{-\infty}^{+\infty} \psi_n^{(+)}(x) dx \\ &= \sqrt{\frac{a}{2\pi\hbar}} \left[ \frac{\sin((n-1/2)\pi - ap/\hbar)}{((n-1/2)\pi - ap/\hbar)} + \frac{\sin((n-1/2)\pi + ap/\hbar)}{((n-1/2)\pi + ap/\hbar)} \right] \\ &= \sqrt{\frac{\Delta p}{2\pi}} \left[ \frac{\sin((p_n - p)/\Delta p)}{(p_n - p)} + \frac{\sin((p_n + p)/\Delta p)}{(p_n + p)} \right] \end{aligned} \quad (16)$$

where  $p_n \equiv (n - 1/2)\pi\hbar/a$  and  $\Delta p \equiv \hbar/a$ . In a classical limit, where we might take  $\hbar \rightarrow 0$  or  $a \rightarrow \infty$  (or at least much larger than any quantum dimension), we have  $\Delta p \rightarrow 0$  and one can show that

$$\lim_{\hbar/a \rightarrow 0} |\phi_n^{(+)}(p)|^2 = \frac{1}{2} [\delta(p - p_n) + \delta(p + p_n)] \quad (17)$$

as expected.

To students first encountering such concepts, however, the use of the mathematical formalism of the Dirac  $\delta$ -function can be less than intuitively obvious, so it would be useful to have an appropriate limiting case where students can see, both physically and mathematically, how the infinite well case is reached. To this end, we consider a variation on the symmetric linear well,  $V(x) = F|x|$ , namely one with infinite walls included, defined via

$$V(x) = \begin{cases} F|x| = V_0|x|/a & \text{for } |x| < a \\ +\infty & \text{for } |x| > a \end{cases}. \quad (18)$$

This potential is sometimes called the 'bouncer on a closed court' [9]. In the limit that  $V_0 \rightarrow 0$ , this potential approaches the symmetric infinite well. We will especially be interested in cases where the energy is greater than  $V_0$  (as in Figs. 3, 4, and 5). In that case, because of the infinite walls, the particle will never slow down and come to rest as it reverses its direction, but rather simply 'bounce' off the infinite wall. In this case, there is not only a maximum value of momentum given by  $p_{(+)} = \sqrt{2mE}$ , but also a minimum value given by  $p_{(-)} = \sqrt{2m(E - V_0)}$ , so that the classical probability density for momenta will only be non-vanishing over the intervals  $(-p_+, -p_-)$  and  $(+p_-, +p_+)$ . The 'half-period',  $\tau$ , required for the position probability density is given by (so long as  $E > V_0$ , as we assume)

$$\begin{aligned} \tau &= \int_{-a}^{+a} \frac{dx}{v(x)} = \int_{-a}^{+a} \frac{dx}{\sqrt{2(E - V_0|x|/a)/m}} \\ &= 2\sqrt{\frac{m}{2}} \left( \frac{4a}{V_0} \right) [\sqrt{E} - \sqrt{E - V_0}] \end{aligned} \quad (19)$$

and the classical period is  $T_{CL} = 2\tau$ . Since the particle achieves the same momentum value twice during each period (due to the symmetry of the well) and  $|F| = V_0/a$ , we can write

$$P_{CL}(p) = \frac{2}{T_{CL}|F(p)|} = \frac{1}{2} \left[ \frac{1}{\sqrt{2mE} - \sqrt{2m(E - V_0)}} \right] = \frac{1}{2} \left[ \frac{1}{p_{(+)} - p_{(-)}} \right] \quad (20)$$

over the two allowed regions and vanishing elsewhere. The complete expression for the



classical probability density for momentum can therefore be written in the form

$$P_{CL}(p) = \begin{cases} \frac{1}{2\Delta p} & \text{for } p_{(-)} \leq |p| \leq p_{(+)} \\ 0 & \text{otherwise} \end{cases} \quad (21)$$

where  $\Delta p \equiv p_{(+)} - p_{(-)}$  and  $P_{CL}(p)$  is clearly normalized appropriately. For fixed values of  $E$  and  $a$ , as we let  $V_0 \rightarrow 0$ , we have  $\Delta p \rightarrow 0$  and we clearly reproduce the  $\delta$ -function structure of the infinite well as the two, isolated rectangular peaks become narrower and higher.

The classical probability density for position can also be easily derived and we find that

$$P_{CL}(x) = \frac{1}{\tau v(x)} = \frac{V_0}{4a[\sqrt{E} - \sqrt{E - V_0}]\sqrt{E - V_0}|x|/a} \quad \text{for } |x| \leq a \quad (22)$$

which has the appropriate limit, namely  $P_{CL}(x) = 1/2a$ , when  $V_0 \rightarrow 0$ .

In order to compare these classical predictions to the corresponding quantum mechanical solutions, we note that the general solutions to the Schrödinger equation for this problem can be written in the form

$$\psi(x) = \begin{cases} C_L Ai(-(x + \sigma)/\rho) + D_L Bi(-(x + \sigma)/\rho) & \text{for } -a \leq x \leq 0 \\ C_R Ai((x - \sigma)/\rho) + D_R Bi((x - \sigma)/\rho) & \text{for } 0 \leq x \leq +a \end{cases} \quad (23)$$

where  $Ai(z)$  and  $Bi(z)$  are standard Airy functions [10] and where we have defined

$$\rho = \left( \frac{\hbar^2 a}{2mV_0} \right)^{1/3} \quad \text{and} \quad \sigma = \frac{Ea}{V_0} \quad (24)$$

We note that symmetry arguments can be used to relate the  $L$  and  $R$  coefficients for the even or odd eigenstates. The divergent  $Bi(z)$  solutions must be used in order to properly match the boundary conditions both at the infinite walls and at the origin. Application of the boundary conditions at  $x = 0$  and  $x = a$ , for example, gives the energy eigenvalue condition for the odd states (where  $\psi(0) = 0$ ) as

$$Ai\left(\frac{-\sigma}{\rho}\right) Bi\left(\frac{a - \sigma}{\rho}\right) - Ai\left(\frac{a - \sigma}{\rho}\right) Bi\left(\frac{-\sigma}{\rho}\right) = 0 \quad (25)$$

and a similar condition for the even eigenstates. The corresponding momentum eigenstates can then be obtained by direct Fourier transform from the allowed  $\psi(x)$ .

As examples of how the limiting case of the infinite well can be approached from the symmetric linear potential, and of how well the classical and quantum probability densities agree (correspondence principle limit), we consider several cases with decreasing values of  $V_0$ .

Specifically, in Figs. 3, 4 and 5, we show examples of solutions (both classical and quantum mechanical) for position- and momentum-space probability densities using Eqns. (21) and (22) for the classical versions and the appropriate quantum solutions. In each case, we have picked an energy corresponding to an allowed quantum eigenstate with  $E \gtrsim 10$  (in scaled units) so that the maximum value of momentum,  $p_{(+)} = \sqrt{2mE}$  is virtually identical in all three cases. In each case we use  $\hbar = 2m = 1$  for simplicity, and choose  $a = 25$ , while varying the values of  $V_0$ . We then show results for  $V_0 = 10$  (Fig. 3),  $V_0 = 6$  (Fig. 4) and  $V_0 = 2$  (Fig. 5) for which the appropriate parameters are shown in Table I.

We note that as  $V_0 \rightarrow 0$ , both the classical and quantum position probability densities,  $P_{CL}(x)$  and  $P_{QM}(x)$ , approach the appropriate 'flat' result for the infinite well: in each case we have used the same vertical scale to show this progression. This limiting behavior of  $\psi(x)$  as  $V_0 \rightarrow 0$  can be examined more rigorously using 'handbook' [10] properties of the  $Ai(z)$  and  $Bi(z)$  functions.

For the case of the momentum densities, the approach to the highly peaked case of the infinite well is also clear, with decreasingly small values of  $\Delta p = p_{(+)} - p_{(-)}$  and increasingly large 'spikes': for these cases, in order to see the detailed structure, we have **not** shown the momentum densities with the same vertical scales (note the axis labeling carefully), but have kept the horizontal axes identical. Interested students can study the systematic variations and correlations between these three cases and may especially notice how the spatial variations in the frequency of zero-crossings in the  $|\psi(x)|^2$  are correlated with the allowed range in momenta.

As a final comment, we note that the 'intrinsic' spread of the two prominent individual peaks in the momentum space probability densities given by Eqn. (16) is of the order of  $\Delta p = \hbar/a$ . This means that when the difference  $\Delta p = p_{(+)} - p_{(-)}$  becomes of this order, the classical description will clearly be a bad representation of the quantum results. In the numerical studies represented in Figs. 3, 4, and 5, with the specific parameters we have used for illustrative purposes, we have  $\Delta p = \hbar/a = 1/25 = 0.04$  which is still substantially smaller than the  $\Delta p = p_{(+)} - p_{(-)}$  values shown in Table I.

## 4. Conclusions

We have examined the structure of classical probability densities for momentum,  $P_{CL}(p)$ , in several simple variations on familiar, one-dimensional potential problems. As our main

example, we have shown how a simple interpolation between the symmetric linear potential and the infinite well, provided by Eqn. (18) can illustrate, in an intuitively attractive and mathematically appropriate manner, how the divergent  $\delta$ -function form of the classical probability density for momentum can arise in the most familiar of all bound state problems, namely the infinite well. Such examples can hopefully provide experience on how to understand and visualize the information content of both classical and quantum mechanical bound state problems found in a momentum-space description of these systems, a topic which is seldom covered in detail in standard undergraduate texts, but which is increasingly important in the modern research literature.

## Acknowledgments

The work of RR was supported, in part, by NSF grant DUE-9950702.

- 
- [1] See, e.g., Park D 1992 *Introduction to the Quantum Theory* (New York: McGraw-Hill) 3rd edition pp 239-241
- [2] Liboff R L 1997 *Introductory Quantum Mechanics* (Reading: Addison-Wesley) 3rd edition pp 192-195
- [3] Robinett R W 1997 *Quantum Mechanics: Classical Results, Modern Systems, and Visualized Examples* (New York: Oxford University Press) pp 110-115
- [4] Cataloglu E and Robinett R W 2001 Testing the development of student conceptual and visualization understanding in quantum mechanics through the undergraduate career (to appear in American Journal of Physics, theme issue on quantum mechanics).
- [5] Hensinger W K *et al.* 2001 Dynamical tunneling of ultracold atoms *Nature* **412** 52-55
- [6] Steck A S *et al.* 2001 Observation of chaos-assisted tunneling between islands of stability *Science* **293** 274-278
- [7] Many references to the 'bouncer' problem in the pedagogical literature can be found in Gea-Banacloche J 1999 A quantum bouncing ball *Am. J. Phys.* **67** pp 410-420
- [8] Robinett R W 1995 Quantum and classical probability distributions for position and momentum *Am. J. Phys.* **63** 823-832
- [9] Aguilera-Navarro V C, Iwamoto H, Ley-Koo E, and Zimerman A H 1981 Quantum bouncer in a closed court *Am. J. Phys.* **49** pp 648-651
- [10] Abramowitz M and Stegun I A 1964 *Handbook of Mathematical Functions* (New York: McGraw-Hill) pp. 446-449

## Tables

$V_0$	$a$	$E$	$p_{(-)}$	$p_{(+)}$	$\Delta p$
10	25	10.066	0.257	3.173	2.916
6	25	10.073	2.108	3.174	1.156
2	25	10.105	2.847	3.179	0.332

**Table I.** Values of potential well parameters for the 'closed-court' potential of Eqn. (18) used in Figs. 3, 4, and 5 respectively. We use  $\hbar = 2m = 1$  in each case. The energy eigenvalues are chosen to be as similar as possible, so that the values of  $p_{(+)}$  are virtually identical in all three cases.

## Figure Captions

Fig. 1. Plot of a generic potential energy function,  $V(x)$  versus  $x$ , which supports bound state motion. A constant value of the total energy,  $E$ , defines the classical turning points  $a, b$ . The corresponding phase-space  $x - p$  plot for the system is shown directly below. The extremal values of momentum,  $\pm p_m = \pm\sqrt{E - V_{min}}$ , correspond to the position of the minimum of the potential energy function. The  $x - p$  phase-space plot is automatically symmetric about the  $p = 0$  axis due to the equal probabilities of finding the particle moving through the same  $dx$  bin, to the left or right, at two different times during its classical period.

Fig. 2. Illustration of the 'projection of trajectory' technique for visualizing the classical probability densities for position (top) and momentum (bottom) for the classical 'bouncer'. Also shown are  $N = 1000$  measurements of the particles position ( $z$ ) and momentum ( $p_z$ ) coordinate, which are consistent with the binned probabilities shown on the vertical  $z(t)$  and  $p_z(t)$  axes.

Fig. 3. Potential energy function (top), classical ( $P_{CL}(x)$ , dashed) and quantum ( $P_{QM}(x) = |\psi(x)|^2$ , solid) position probability densities (middle), and classical ( $P_{CL}(p)$ , dashed) and quantum ( $P_{QM}(p) = |\phi(p)|^2$ , solid) momentum probability densities (bottom) for the symmetric linear well with infinite wall potential in Eqn. (18) with  $V_0 = 10$ . The values of the other parameters are shown in Table I.

Fig. 4. Same as Fig. 3, but with  $V_0 = 6$ . Note that the vertical axis for the  $P_{CL}(p), P_{QM}(p)$  plot is not the same as in Figs. 3 or 5.

Fig. 5. Same as Fig. 3, but with  $V_0 = 2$ . Note that the vertical axis for the  $P_{CL}(p), P_{QM}(p)$  plot is not the same as in Figs. 4 or 5.

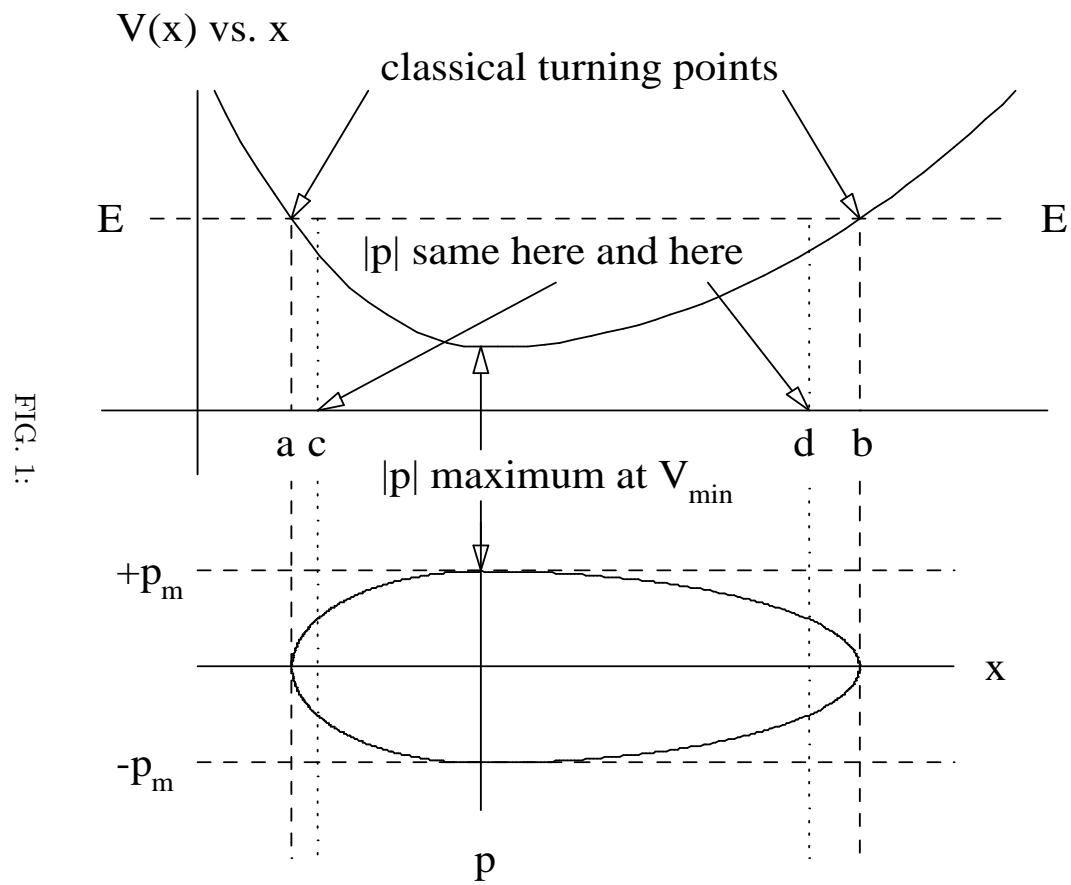
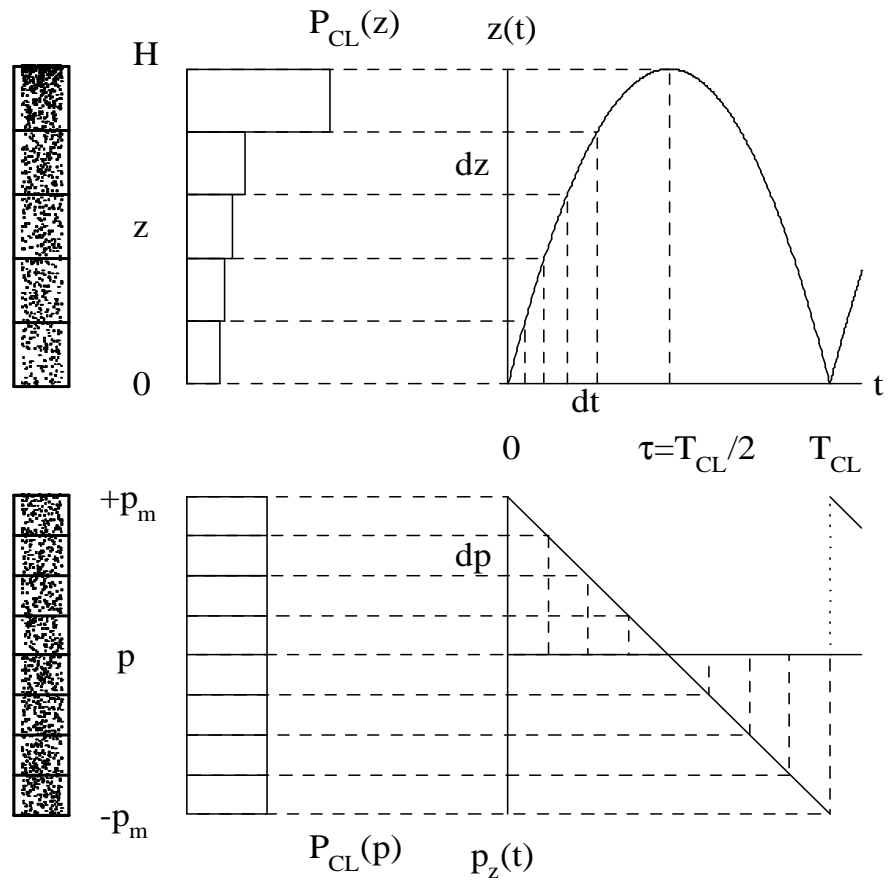


FIG. 2.





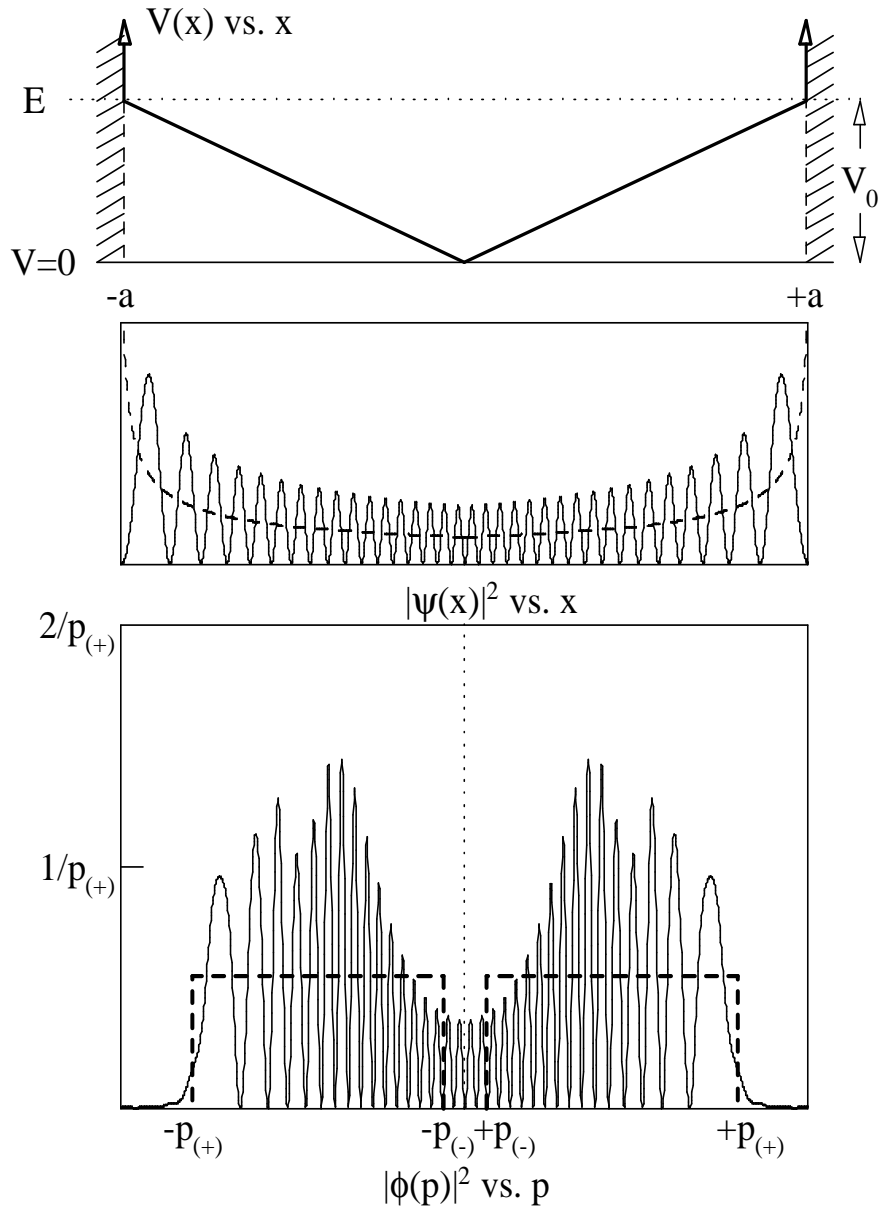


FIG. 3:

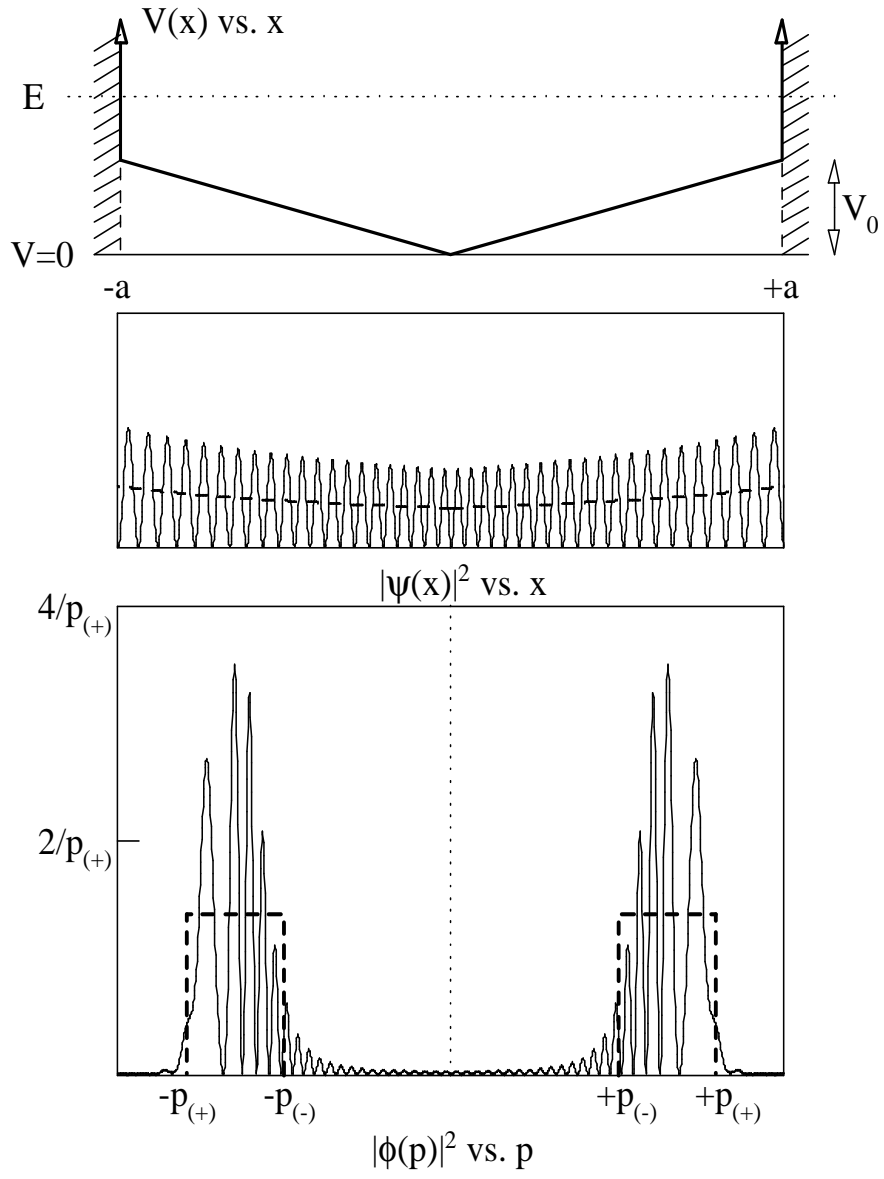


FIG. 4:

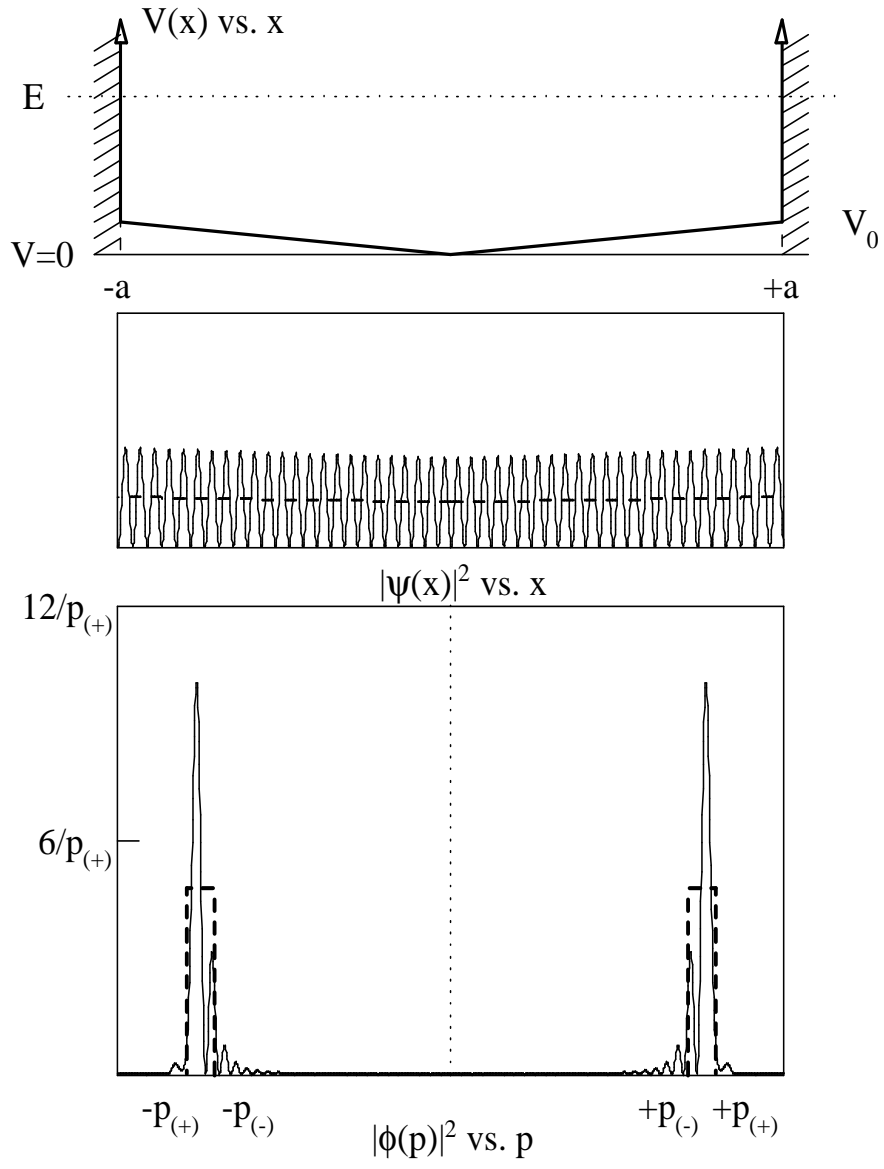


FIG. 5: